



SEARCH FOR SECOND-CLASS CURRENTS IN THE DECAY

$$\tau^- \rightarrow \pi^- \omega \nu_\tau$$

The *BABAR* Collaboration

Tim West

The University of Manchester

Tau08 Workshop

23 September 2008

- ⇒ The *BABAR* detector
- ⇒ Second-class currents
- ⇒ Previous results
- ⇒ Data samples
- ⇒ Analysis method
- ⇒ Event selection
- ⇒ Background events
 - Non-resonant background events
 - Resonant $e^+e^- \rightarrow q\bar{q}$ background events
 - Resonant $\tau^+ \tau^-$ background events
- ⇒ Efficiency
- ⇒ Result and final fit
- ⇒ Systematic uncertainties
- ⇒ Results and conclusions

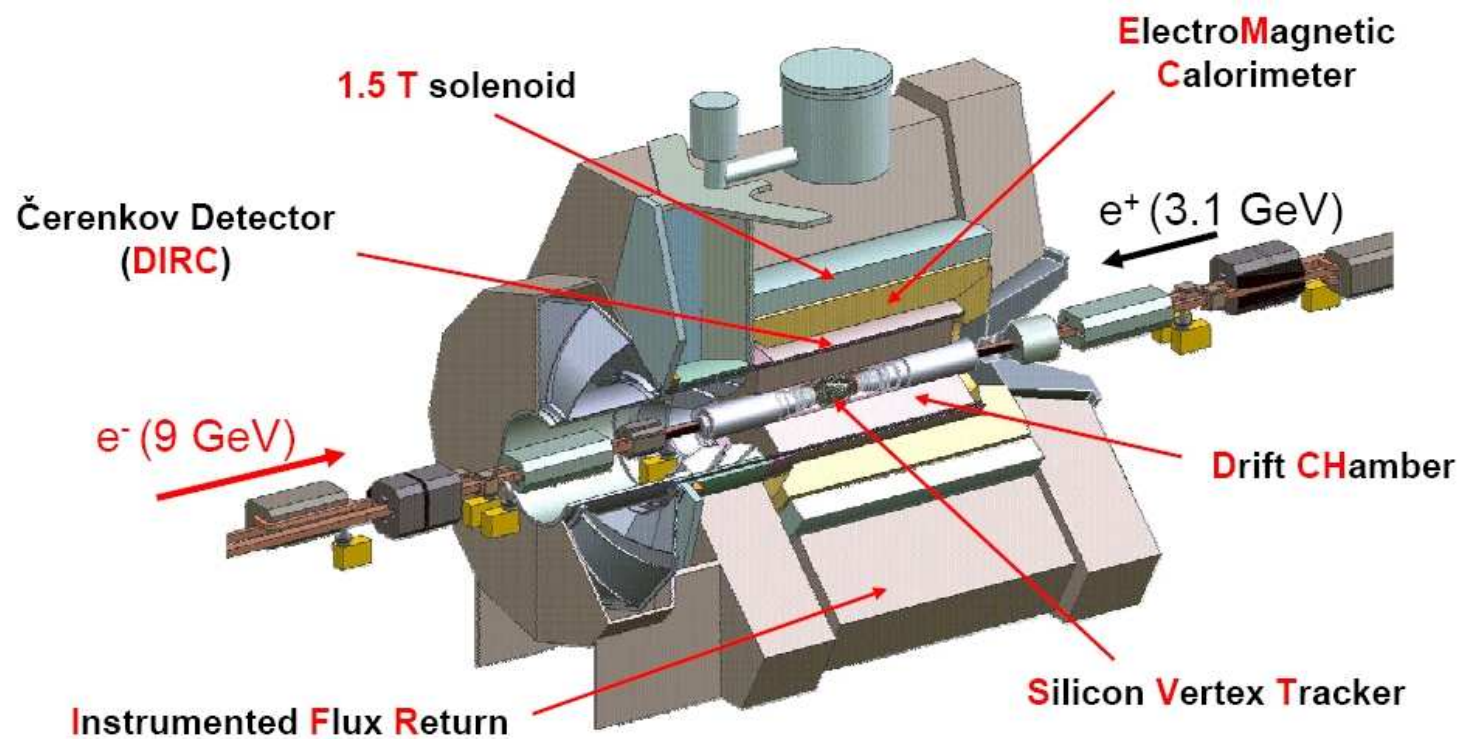


Figure 1: Schematic view of the *BABAR* detector.

- ⇒ Weak currents can be classified dependent on their G-parity
S. Weinberg, Phys. Rev. 112 (1958).
 - G-parity is an extension of charge conjugation to include strong isospin multiplets as eigenstates:

$$\hat{G} = \hat{C}e^{i\pi\hat{I}_2}.$$
- ⇒ Classify them as:
 - First-class (FCC), with $PG(-1)^J = +1$ ($J^{PG} = 0^{++}, 0^{--}, 1^{+-}, 1^{-+}$),
 - Second-class (SCC), with $PG(-1)^J = -1$ ($J^{PG} = 0^{+-}, 0^{-+}, 1^{++}, 1^{--}$).
- ⇒ Previous searches for second-class currents in τ decays and nuclear β decay
 - No confirmed evidence of second-class currents.
- ⇒ In the Standard Model, the decay constants associated with SCC are proportional to the $u-d$ quark mass difference.

- ⇒ The decay $\tau^- \rightarrow b_1^-(1235)\nu_\tau \rightarrow \pi^- \omega \nu_\tau$ would be a SCC with $J^{PG} = 1^{++}$ (axial-vector current).
- ⇒ The decay $\tau^- \rightarrow \pi^- \omega \nu_\tau$ also occurs through a FCC with $J^{PG} = 1^{-+}$ (vector current) — $\mathcal{B}(\tau^- \rightarrow \pi^- \omega \nu_\tau) \sim 2\%$ (PDG).
- ⇒ Limits are placed in terms of

$$\frac{N^{\pi\omega}(\text{non-vector})}{N^{\pi\omega}(\text{vector})}.$$

- ⇒ Current limits are from
 - CLEO: $< 6.4\%$ at the 95% CL
K. E. Edwards et al., Phys. Rev. D61, 072003 (2000),
 - ALEPH: $< 8.6\%$ at the 95% CL
D. Buskulic et al., Zeit. Phys. C74, 263 (1997).
- ⇒ No theoretical predictions for the level of SCC in this decay.

Data sample

- ⇒ On-peak data from Run 1 to Run 5, 347 fb^{-1} (319 million $\tau^+ \tau^-$ pairs).

MC sample

- ⇒ $e^+e^- \rightarrow \tau^+\tau^-$ simulated by KK2F, τ decays by TAUOLA, $q\bar{q}$ by EvtGen, FSR by Photos, detector simulation uses GEANT4
- ⇒ Generic $\tau^+ \tau^-$ MC includes:
 - $\tau^- \rightarrow \pi^- \omega \nu_\tau$ with $J^{PG} = 1^{+-}$,
 - $\tau^- \rightarrow \pi^- \pi^0 \omega \nu_\tau$ — main background.

ANALYSIS METHOD (1)

- ⇒ Reconstruct $\tau^- \rightarrow \pi^- \omega \nu_\tau$, where $\omega \rightarrow \pi^+ \pi^- \pi^0$.
- ⇒ Obtain the $\cos \theta_{\omega\pi}$ spectrum for $\tau^- \rightarrow \pi^- \omega \nu_\tau$ decays, where $\theta_{\omega\pi}$ is defined as the angle between the π^- and the normal to the ω decay plane in the ω rest frame (Fig. 2).
- ⇒ The FCC has $J^P = 1^-$ and $L = 1$.
- ⇒ The SCC has $J^P = 1^+$ and $L = 0, 2$ or $J^P = 0^-$ and $L = 1$.
- ⇒ The different $J^P(L)$ combinations produce different angular distributions (Fig. 3).

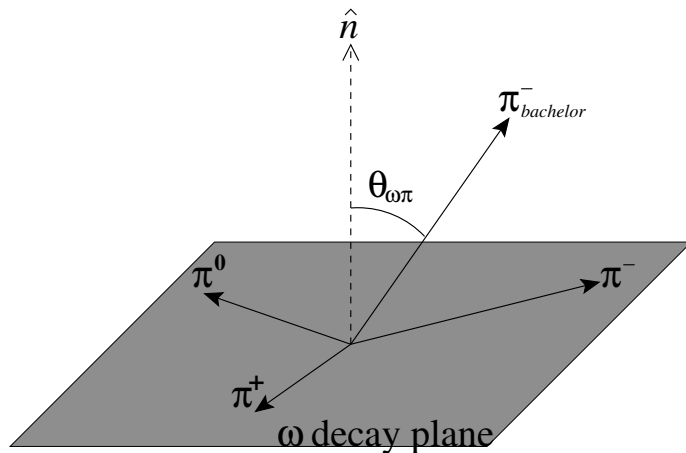


Figure 2: Definition of the angle $\theta_{\omega\pi}$.

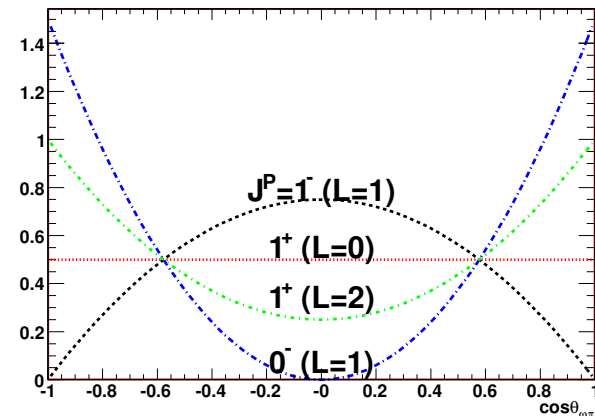


Figure 3: Angular distributions for different $J^P(L)$ states. Normalization of functions is arbitrary.

ANALYSIS METHOD (2)

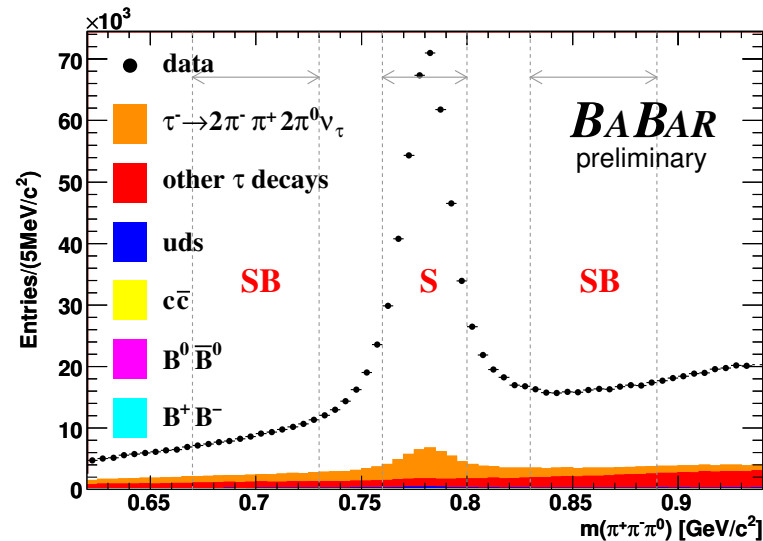


Figure 4: $m(\pi^+ \pi^- \pi^0)$ spectrum with one π^0 requirement with **S**ignal and **S**ide**B**and regions marked.

- ⇒ Obtain $\cos \theta_{\omega\pi}$ spectrum for data in signal region.
- ⇒ Subtract contribution from combinatoric backgrounds using sidebands.
- ⇒ Subtract contribution from $\tau^+ \tau^-$ and $q\bar{q}$ backgrounds using a combination of data and MC.
- ⇒ Correct for any variation in efficiency as a function of $\cos \theta_{\omega\pi}$.
- ⇒ Fit this final $\cos \theta_{\omega\pi}$ spectrum to obtain a SCC measurement.

SELECTION CRITERIA

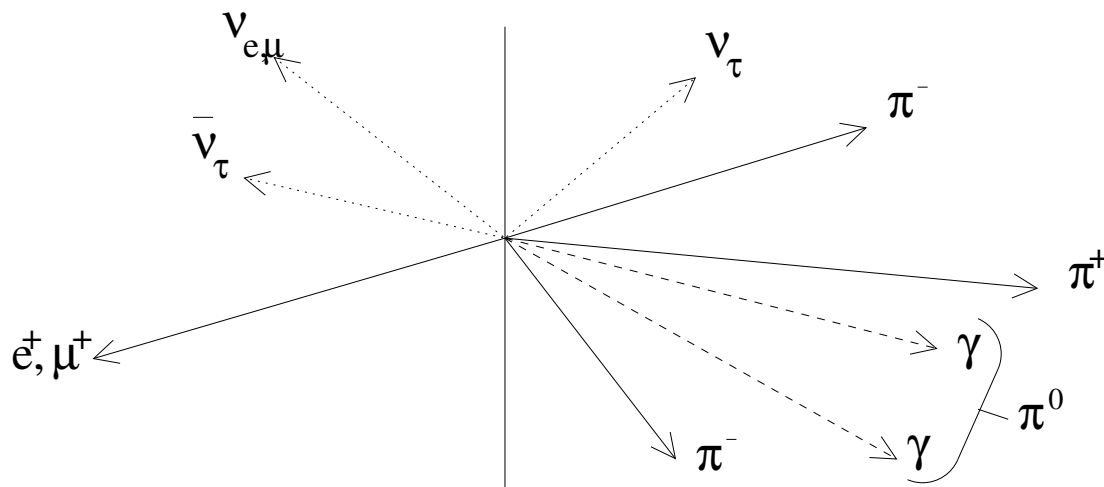


Figure 5: Required topology.

- ⇒ Divide events into two hemispheres using thrust and require a 1-3 topology with at least one π^0 candidate ($100 \text{ MeV}/c^2 < m(\gamma\gamma) < 160 \text{ MeV}/c^2$) on the 3-prong side.
- ⇒ Event level cuts (thrust, energy etc.) to select $\tau^+ \tau^-$ events.
- ⇒ 1-prong charged track required to pass electron or muon selection criteria.
- ⇒ 3-prong charged tracks required to pass pion selection criteria.

- ⇒ Make two final samples, one for looking at the signal $\tau^- \rightarrow \pi^- \omega \nu_\tau$ decays, the other for studying the main background, $\tau^- \rightarrow \pi^- \pi^0 \omega \nu_\tau$. For the signal sample:
 - Require only one π^0 in the signal hemisphere,
 - No left over photons in the signal hemisphere that are not associated with a charged track,
 - $m(\pi^- \pi^+ \pi^- \pi^0) < 1.777 \text{ GeV}/c^2$.
- ⇒ For the $\tau^- \rightarrow \pi^- \pi^0 \omega \nu_\tau$ sample:
 - Reconstruct two unique π^0 candidates (no common photons) in the signal hemisphere.
 - $m(\pi^- \pi^+ \pi^- \pi^0 \pi^0) < 1.777 \text{ GeV}/c^2$.
- ⇒ Final selection rates are:
 - 2.96% for $\tau^- \rightarrow \pi^- \omega \nu_\tau$ in one π^0 sample,
 - 0.70% for $\tau^- \rightarrow \pi^- \pi^0 \omega \nu_\tau$ in one π^0 sample,
 - 1.26% for $\tau^- \rightarrow \pi^- \pi^0 \omega \nu_\tau$ in two π^0 sample,

- ⇒ Use sidebands in data to model $\cos \theta_{\omega\pi}$ for combinatoric backgrounds in the signal region (Fig. 6).
- ⇒ Use MC to model ω resonance in $q\bar{q}$ backgrounds:
 - ➔ Compare data and MC events with $m(\pi^- \pi^+ \pi^- \pi^0) > 2.1 \text{ GeV}/c^2$ to check the $q\bar{q}$ events have the correct normalization.
 - ➔ Use sideband sideband subtraction on the $q\bar{q}$ MC to obtain $\cos \theta_{\omega\pi}$ spectra for ω resonant events (Fig. 7).

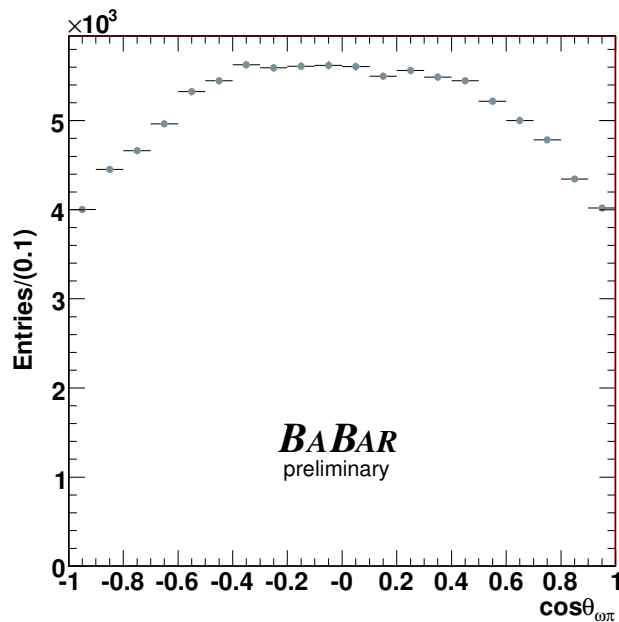


Figure 6: $\cos \theta_{\omega\pi}$ spectrum for data sidebands.

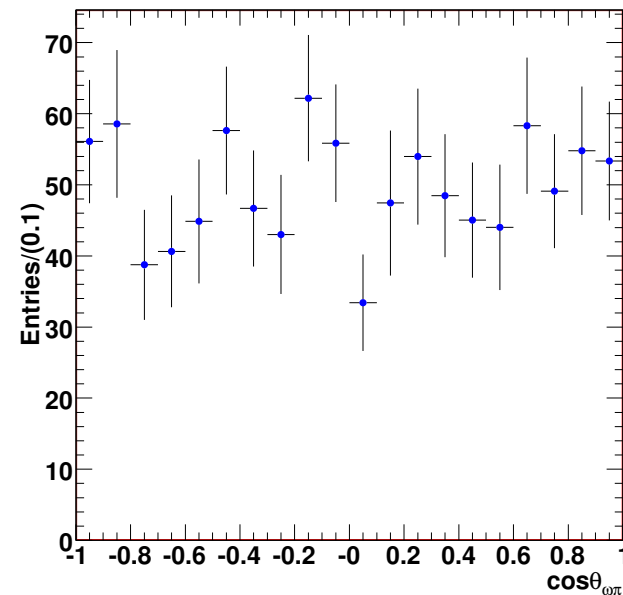


Figure 7: $\cos \theta_{\omega\pi}$ spectrum for ω resonant $q\bar{q}$ events from MC.

⇒ Other τ decays that may be present in the final sample:

→ $\tau^- \rightarrow \pi^- \pi^0 \omega \nu_\tau$

→ $\tau^- \rightarrow K^- \omega \nu_\tau$

→ $\tau^- \rightarrow \pi^- \pi^0 \pi^0 \omega \nu_\tau$

→ $\tau^- \rightarrow \pi^- \pi^+ \pi^- \omega \nu_\tau$

⇒ Of these, $\tau^- \rightarrow \pi^- \pi^0 \omega \nu_\tau$ contributes the most events; of the 394,000 ω resonant events in the data, ($\sim 5\%$) from $\tau^- \rightarrow \pi^- \pi^0 \omega \nu_\tau$, compared to $< 0.2\%$ total for the others ($q\bar{q}$ is $< 0.4\%$).

⇒ $\tau^- \rightarrow \pi^- \pi^0 \omega \nu_\tau$ events are not well modeled in the MC; both the $\cos \theta_{\omega\pi}$ spectra and the branching fraction are incorrect:

→ The data and MC samples with the requirement of one additional π^0 are used to obtain the correct $\cos \theta$ spectrum for $\tau^- \rightarrow \pi^- \pi^0 \omega \nu_\tau$ decays.

- ⇒ Use $m(\pi^+ \pi^- \pi^0)$ spectrum with an additional π^0 required (Fig. 8) to correct branching fraction in MC for $\tau^- \rightarrow \pi^- \pi^+ \pi^- \pi^0 \pi^0 \nu_\tau$.
- ⇒ Use $\cos \theta_{\omega\pi}$ spectrum with an additional π^0 required (Fig. 9) to correct angular spectrum in MC for $\tau^- \rightarrow \pi^- \pi^+ \pi^- \pi^0 \pi^0 \nu_\tau$.

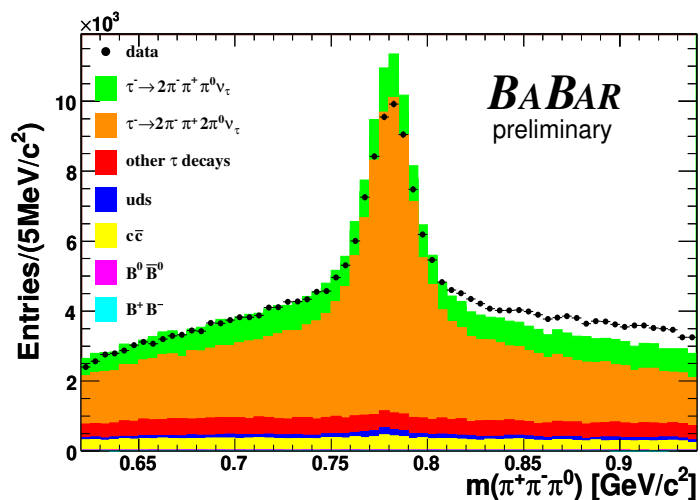


Figure 8: $m(\pi^+ \pi^- \pi^0)$ for data and MC with $2\pi^0$ requirement.

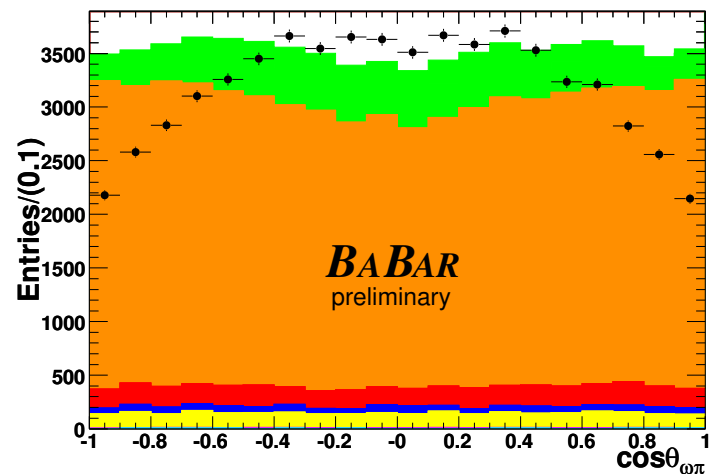


Figure 9: $\cos \theta_{\omega\pi}$ spectra for data and MC with $2\pi^0$ requirement.

$\tau^- \rightarrow \pi^- \pi^0 \omega \nu_\tau$ BACKGROUND (2)

- ⇒ Carry out sideband and background subtractions on the data with the additional π^0 requirement to obtain the correct $\cos \theta_{\omega\pi}$ spectrum for $\tau^- \rightarrow \pi^- \pi^0 \omega \nu_\tau$ decays, shown in Fig. 10.

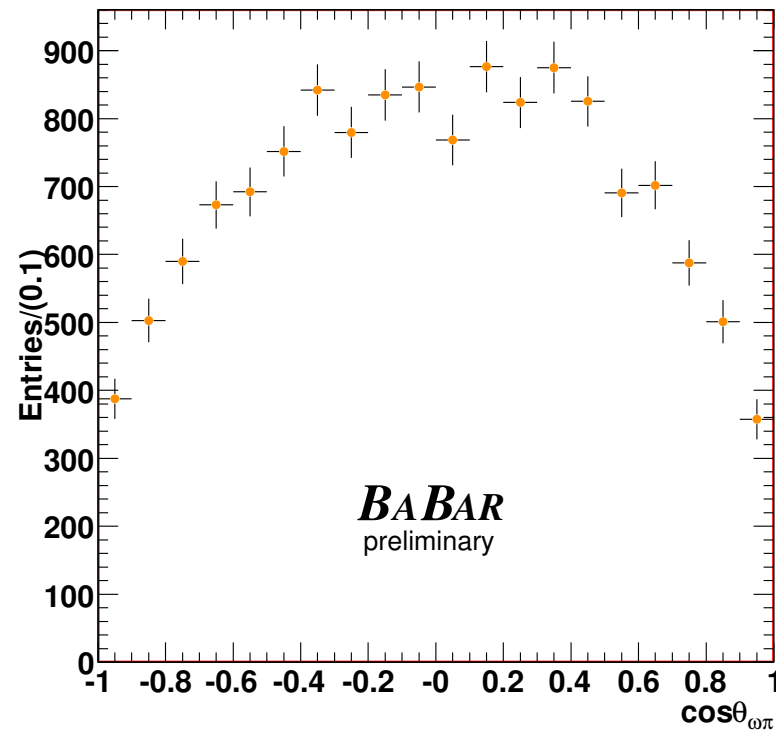


Figure 10: Corrected $\cos \theta_{\omega\pi}$ spectrum for $\tau^- \rightarrow \pi^- \pi^0 \omega \nu_\tau$ decays.

- ⇒ The $\cos \theta_{\omega\pi}$ spectrum obtained after the backgrounds have been subtracted off is corrected for any efficiency variation as a function of $\cos \theta_{\omega\pi}$.
- ⇒ Efficiency histogram is obtained from MC.

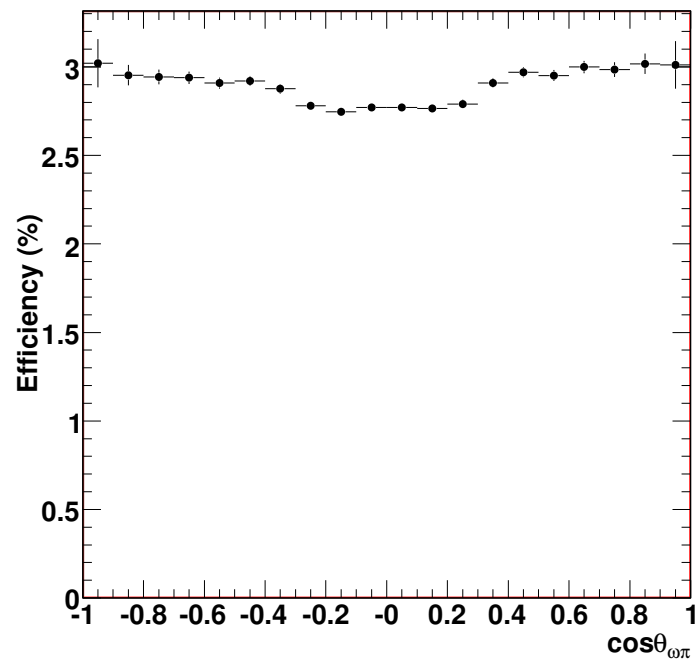
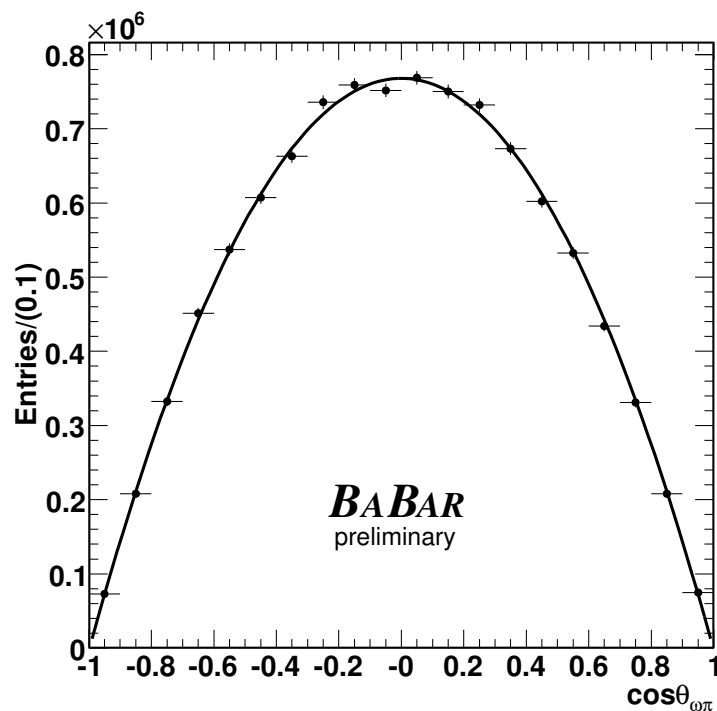


Figure 11: Efficiency as a function of $\cos \theta_{\omega\pi}$ from MC.



arXiv:0807.4900 [hep-ex]

Figure 12: Data fit to find SCC contribution. $\chi^2/dof = 15.4/18$.

⇒ The final fit uses the function

$$F(\cos\theta_{\omega\pi}) = N[(1 - \epsilon)F^{FCC}(\cos\theta_{\omega\pi}) + \epsilon F_{L=0}^{SCC}(\cos\theta_{\omega\pi})],$$

where $F^{FCC}(x) \propto (1 - x^2)$ and $F_{L=0}^{SCC}(x) \propto (1)$, to find the second class current fraction, ϵ .

⇒ The result from the fit is $\epsilon = (-5.5 \pm 5.8(\text{stat.})) \times 10^{-3}$.

⇒ Correction applied for $\mathcal{B}(\tau^- \rightarrow \pi^- \pi^0 \omega \nu_\tau)$ $\sigma_\epsilon = \pm 0.0007$,

⇒ un-modeled resonant τ decays:

→ $\tau^- \rightarrow K^- \omega \nu_\tau$,

→ $\tau^- \rightarrow \pi^- \pi^+ \pi^- \omega \nu_\tau$,

→ $\tau^- \rightarrow \pi^- \pi^0 \pi^0 \omega \nu_\tau$,

total contribution is $\sigma_\epsilon = {}^{+0.0000}_{-0.0055}$,

⇒ $q\bar{q}$ normalization $\sigma_\epsilon = \pm 0.0001$,

Total systematic error is $\sigma_\epsilon = {}^{+0.0008}_{-0.0055}$.



RESULTS AND CONCLUSIONS

- ⇒ Final result from fit for second-class current contribution is

$$\epsilon = (-5.5 \pm 5.8(\text{stat.})_{-5.5}^{+0.8}(\text{syst.})) \times 10^{-3}.$$

- ⇒ This sets limits on

$$\frac{N^{\omega\pi(\text{non-vector})}}{N^{\omega\pi(\text{vector})}} = \frac{\epsilon}{1 - \epsilon}$$

of **0.69%** at 90% C.L. and **0.85%** at 95% CL (using a Bayesian scheme).

- ⇒ Order of magnitude improvement over previous limits.
- ⇒ Equivalent to $\mathcal{B}(\tau^- \rightarrow \pi^- \omega \nu_\tau(\text{second-class})) < 1.3 \times 10^{-4}$ at 90% C.L.
- ⇒ Analysis is presented in [arXiv:0807.4900 \[hep-ex\]](https://arxiv.org/abs/0807.4900).

BACKUP SLIDE(S)

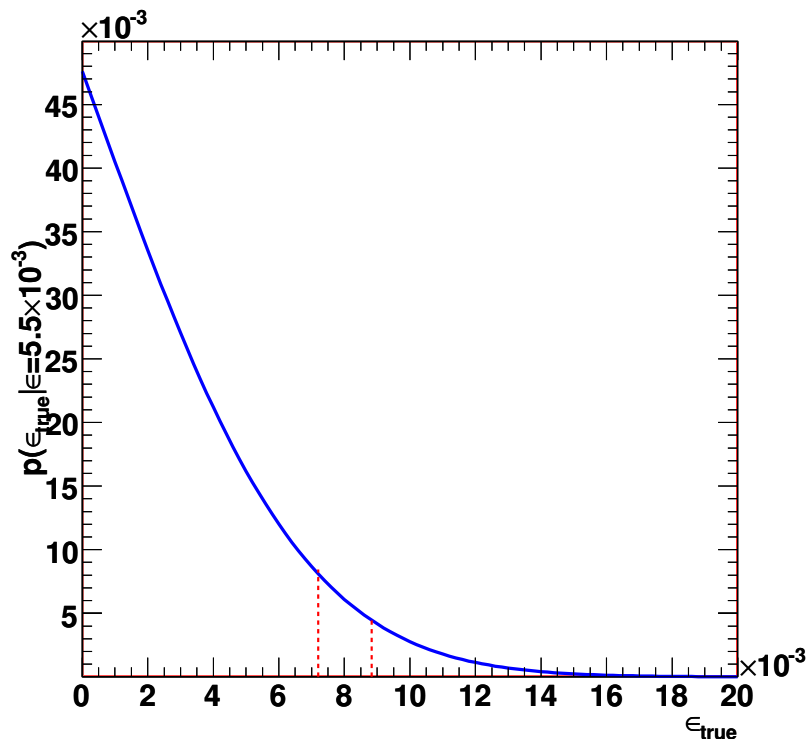


Figure 13: $p(\epsilon_{true}|\epsilon)$ — Bayesian limit.

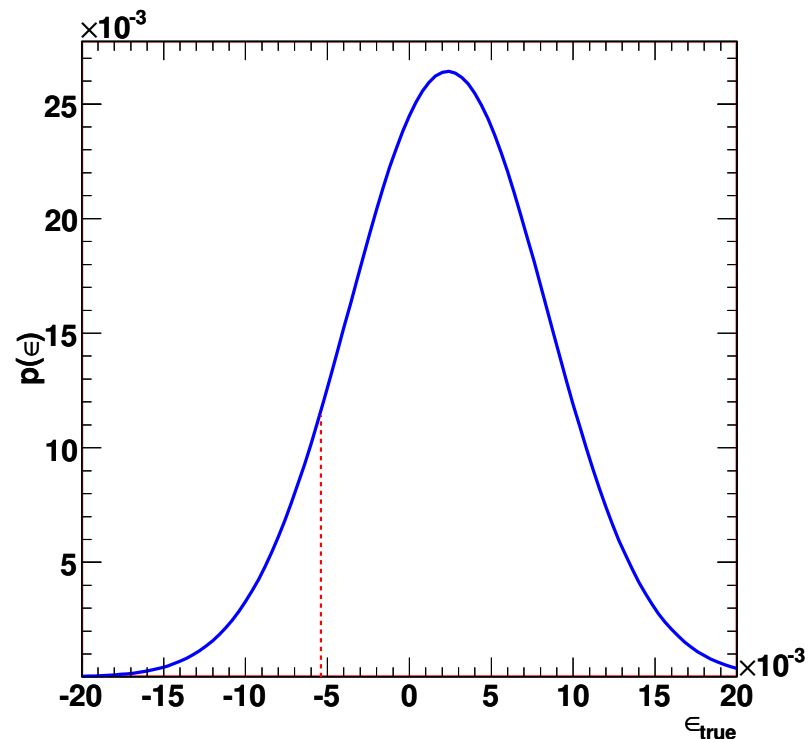


Figure 14: $p(\epsilon)$ — classical limit.

Limits on $N^{\omega\pi}(\text{non-vector})/N^{\omega\pi}(\text{vector})$:

- ⇒ Bayesian limits are 0.69% (90% CL) and 0.85% (95% CL).
- ⇒ Classical limits are 0.20% (90% CL) and 0.42% (95% CL).